49th IEEE Conference on Decision and Control
December 15-17, 2010
Hilton Atlanta Hotel, Atlanta, GA, USA

# A Control Theoretic Approach to Robot-Assisted Locomotor Therapy

Robert D. Gregg, Timothy W. Bretl, and Mark W. Spong

*Abstract*— **This paper proposes a control theoretic strategy for human walking gait assistance based on *underactuated potential energy shaping*. We design a simple control law that lessens the perceived weight of the patient's center of mass through a robotic ankle-foot orthosis (AFO) with one actuated degree-of-freedom. We then adopt a passive "compass-gait" bipedal walker as an implicit model of human locomotor behavior, which we simulate to draw beneficial implications for rehabilitation such as energy regulation, improved stability, and progressive training by Lyapunov funneling. Given current challenges in developing effective robot-assisted locomotor therapies, this paper offers a novel systematic approach to control strategy design for gait training and at-home assistance.**

## I. Introduction

The field of therapeutic robotics has shown great promise in treating neuromotor disorders and alleviating the intensive labor required by physical therapists [1]. However, significant challenges still remain with the design of robot-assisted control strategies for locomotor rehabilitation. Recent studies with the Lokomat exoskeleton suggest that strategies imposing reference gait patterns (i.e., joint position trajectories) are less effective than manual therapy in terms of recovered walking speed and endurance for subacute and chronic stroke patients [2], [3]. In the case of robotic ankle-foot orthosis (AFO), torque profiles are typically tuned in an ad hoc manner based on how a healthy walking gait *should* look. This requires active estimation of the intended modality (e.g., walking or standing) and the phase of a gait cycle, which are prone to errors that risk life-threatening falls. Costly attention must also be given to adapting these control sequences to individual morphology and impairment. It is clear that novel systematic approaches are needed for control strategy design based on fundamental principles of locomotion.

Recently developed AFO devices such as the Anklebot [4] and Portable Powered Ankle-Foot Orthosis (PPAFO) [5] present an opportunity to implement and evaluate novel strategies for both clinical and at-home therapy. The low-friction, backdriveable Anklebot employs an impedance controller based on proportional-derivative gains that can be tuned to force or measure ankle stiffness. However, uncertainty in the human-machine feedback loop (the human control policy is essentially a "black box") prevents model-based analysis on how such strategies influence walking and motor recovery. The *underactuated*[1] nature of ankle control in the overall human-machine system presents yet another challenge to control policy design. Fortunately, the body of literature concerning *dynamic* robot walking and control may inspire some new solutions.

### A. Dynamic Walking Robots to Human Rehabilitation

Dynamic walking is the fast and energy-efficient form of locomotion based on "controlled falling." During every step cycle, the body's center of mass (COM) engages in a gravity-powered fall along a pendular arc until foot-ground impact redirects this motion into the next cycle [6]. In terms of a biped's joint trajectories, this produces attractive periodic orbits called *limit cycles*.

Stable limit cycles have been shown to exist down shallow slopes for "passive" robot walkers without any control or actuation whatsoever [7]–[9]. The potential energy provided by gravity at every step is fundamental to this natural motion. This fact has been exploited by robot control strategies that shape the potential energy into different forms, such as rotating the gravity vector to enable pseudo-passive dynamic walking on arbitrary slopes [10], [11]. These gaits do not track reference trajectories, but naturally appear as a result of system nonlinearities.

In terms of human dynamic locomotion, evolution has given us the bipedal morphology to outwalk quadrupeds over long distances [12]. Minetti et al. found that the metabolic energetic cost of walking is minimized on shallow decline slopes [13], showing that humans similarly exploit potential energy provided by gravity. This suggests that passive walking models might relate human locomotor principles to guide the design and analysis of robot-assisted therapies. Moreover, speed-intensive locomotor training is known to increase gait efficiency and muscle activation for hemiparetic[2] patients [14], demonstrating the importance of passive dynamics in locomotor therapy.

Therefore, we propose that assistive control strategies should *enable* and *encourage* the pendular/ballistic nature of human walking. This paper develops a design methodology for locomotor therapy that alters dynamical characteristics of the human system using *underactuated potential energy shaping*. In particular, we design a control theoretic strategy for the PPAFO that lessens the perceived weight of the patient's COM, thus belonging to the "counterbalancing" category of assistive controllers [15].

R. D. Gregg is with the Department of Electrical and Computer Engineering, and T. Bretl is with the Department of Aerospace Engineering, University of Illinois at Urbana-Champaign, Urbana, IL 61801 {rgregg,tbretl}@illinois.edu

M. W. Spong is with the Department of Electrical Engineering, University of Texas at Dallas, Richardson, TX 75080 mspong@utdallas.edu

This research was partially supported by NSF Grants CMMI-0856368, CMS-0510119, and NSF-0931871.

[1]The human-machine system has many more degrees-of-freedom than degrees of actuator control. Therefore, it is said to be *underactuated*.

[2]Weakness in one side of the body, often caused by stroke.

### B. Related Work

This work relates to new control strategies for the Lokomat exoskeleton that define potential force fields around reference trajectories [16]. This method of *generalized elasticities* maximizes robot transparency when the patient follows the predefined trajectory, otherwise providing active support and guidance. Our approach instead shapes the gravitational potential energy to modify the dynamical behavior of the human-in-the-loop. Using no reference trajectories, this produces simple control policies that are compliant to patient intent and easily tuned for personalized therapy. This embraces PPAFO mobility [5] and remains transparent to the human's passive dynamics, overcoming the shortfalls of mechatronic harnesses [17] and gravity-canceling exoskeletons [18].

## II. Lagrangian Mechanics

The Lagrangian formulation of mechanical system dynamics is fundamentally related to system energetics and therefore will be useful in our control design. The configuration of a $n$-degree of freedom (DOF) mechanical system is given by the vector $q$ of generalized coordinates in configuration space $\mathcal{Q}$. The system dynamics are described by the state pair $(q, \dot{q})$ in tangent bundle[3] $T\mathcal{Q}$, by which the *Lagrangian* function $\mathcal{L} : T\mathcal{Q} \to \mathbb{R}$ is given as

$$\begin{aligned} \mathcal{L}(q,\dot{q}) &= \mathcal{K}(q,\dot{q}) - \mathcal{V}(q) \\ &= \frac{1}{2}\dot{q}^T M(q)\dot{q} - \mathcal{V}(q), \end{aligned} \tag{1}$$

where $\mathcal{K}(q, \dot{q})$ is the kinetic energy, $\mathcal{V}(q)$ is the potential energy, and $M(q)$ is the $n \times n$ generalized mass/inertia matrix. By the least action principle, system integral curves necessarily satisfy the *Euler-Lagrange* (E-L) equations

$$\frac{d}{dt}\nabla_{\dot{q}}\mathcal{L} - \nabla_q \mathcal{L} = \tau, \tag{2}$$

where vector $\tau$ contains the generalized external torques. This system of second-order ordinary differential equations directly gives the dynamical equations of motion in phase space $T\mathcal{Q}$. These equations have the special structure

$$M(q)\ddot{q} + C(q,\dot{q})\dot{q} + N(q) = Su, \tag{3}$$

where $n \times m$ matrix $S$ maps $m$-dimensional control input $u$ to the $n$-dimensional generalized torques, $n \times n$-matrix $C$ contains the Coriolis/centrifugal terms, and vector $N = \nabla_q \mathcal{V}$ contains the potential torques.

## III. Underactuated Potential Shaping

It is often desirable to use control to "shape" the potential energy of a mechanical system, i.e., replace $\mathcal{V}$ with some $\widetilde{\mathcal{V}}$ that has beneficial properties. In the case of underactuated control (when $m < n$), matrix $S$ is not invertible, so only a particular set of energies are achievable from the range space of $S$. This has been well studied in the literature (e.g., [19], [20]) in terms of energy *matching conditions*. Given continuous dynamics (3) and desired $\widetilde{N} = \nabla_q \widetilde{\mathcal{V}}$, we need

$$\begin{aligned} 0 &= M(q)\ddot{q} + C(q,\dot{q})\dot{q} + N(q) - Su \\ &= M(q)\ddot{q} + C(q,\dot{q})\dot{q} + \widetilde{N}(q), \end{aligned} \tag{4}$$

which is equivalent to the necessary condition

$$Su = N(q) - \widetilde{N}(q). \tag{5}$$

We must characterize the null space of $S$, so we define the full rank *left-annihilator* $S^\perp$ such that $S^\perp S = 0$. Then, the right-hand side of (5) is in the range space of $S$ if:

$$S^\perp \left( N(q) - \widetilde{N}(q) \right) = 0, \ \forall\, q \in \mathcal{Q} \tag{6}$$

This allows us to apply a left pseudo-inverse to (5) to derive the underactuated control that exactly achieves potential $\widetilde{V}$:

$$u = (S^T S)^{-1} S^T \left( N(q) - \widetilde{N}(q) \right). \tag{7}$$

On the other hand, underactuated *kinetic* energy shaping involves nonlinear partial differential equations corresponding to matching conditions in addition to (6). These are very difficult to solve (cf. [19]), but we will argue that only *potential* shaping is necessary for ankle-foot orthosis.

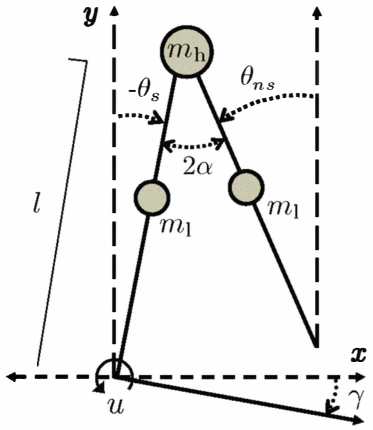


Fig. 1. Model diagram for the planar compass-gait biped. The AFO at the stance ankle (assumed massless for simplicity) applies joint torque $u$.

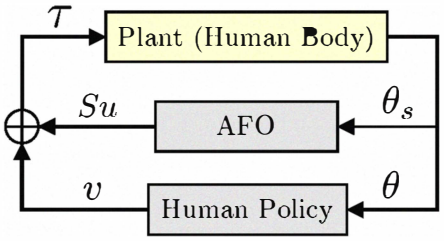


Fig. 2. Human-AFO feedback loop. Note that $v = 0$ for passive walking.

## IV. Application to Ankle-Foot Orthosis

In the absence of reliable models for human control policies, we adopt the passive "compass-gait" biped (Fig. 1) as the human plant in the control loop of Fig. 2. This uncontrolled biped is known to naturally have passive limit

[3]The space of configurations and their tangential velocities.

cycles down shallow slopes, which are governed by pendular single-support dynamics similar to that of human walking. By studying the effect of AFO control strategies on passive walking gaits, we can predict some practical implications for assisted human walking and locomotor therapy.

### A. Biped Model

The compass-gait biped has point feet that exactly coincide with the ankle joints. This simple model's 2-DOF configuration is given by vector $\theta = (\theta_{\rm s}, \theta_{\rm ns})$ in configuration space $\mathcal{Q} = \mathbb{T}^2$, representing the stance angle at the ankle and the non-stance/swing angle at the hip. The single-support phase dynamics are represented by continuous system (3) with

$$M(\theta) = \begin{pmatrix} \frac{l^2}{4}(5m_{\rm l} + 4m_{\rm h}) & -\frac{l^2 m_{\rm l}}{2}\cos(\theta_{\rm s} - \theta_{\rm ns}) \\ -\frac{l^2 m_{\rm l}}{2}\cos(\theta_{\rm s} - \theta_{\rm ns}) & \frac{l^2 m_{\rm l}}{4} \end{pmatrix}$$

$$C(\theta, \dot{\theta}) = \frac{l^2 m_{\rm l}}{2}\begin{pmatrix} 0 & -\dot{\theta_{\rm ns}}\sin(\theta_{\rm s} - \theta_{\rm ns}) \\ \dot{\theta}_{\rm s}\sin(\theta_{\rm s} - \theta_{\rm ns}) & 0 \end{pmatrix}$$

and of particular interest, the potential energy

$$V(\theta) = -\frac{1}{2}gl(m_{\rm l}\cos(\theta_{\rm ns}) - (3m_{\rm l} + 2m_{\rm h})\cos(\theta_{\rm s})) \quad (8)$$

yields the potential torque vector

$$N(\theta) = \nabla_\theta V = \begin{pmatrix} -gl(3m_{\rm l} + 2m_{\rm h})\sin(\theta_{\rm s})/2 \\ glm_{\rm l}\sin(\theta_{\rm ns})/2 \end{pmatrix}. \quad (9)$$

The abstract application of AFO to the stance ankle (assumed massless for simplicity) provides underactuated control ($m = 1$) through input $u$ with torque map $S = \begin{pmatrix} 1 & 0 \end{pmatrix}^T$ in system (3), where we assume torques are applied against ground without slipping. This approximates human ankle behavior while the foot is in flat contact with ground, which is valid for certain phases of a human walking cycle (we will return to this later). We fit both ankles with AFO to have symmetry[4] between each leg's stance cycle. We do not consider active AFO control during swing phase, since this has no effect on the dynamics of our model.

The continuous-time single-support phase is defined by unilateral constraint $h(\theta) \geq 0$, where scalar

$$h(\theta) = l((\cos(\theta_{\rm s}) - \cos(\theta_{\rm ns})) + (\sin(\theta_{\rm s}) - \sin(\theta_{\rm ns}))\tan(\gamma))$$

gives the height of the swing foot above ground with slope angle $\gamma$. The instantaneous impact event from foot-ground strike is indicated by the *guard* condition[5] characterized by switching surface

$$G \;=\; \{(\theta, \dot{\theta}) | h(\theta) = 0,\; \dot{h} = (\nabla_\theta h)\dot{\theta} < 0\} \;\subset\; T\mathcal{Q}.$$

We model these impulsive events as perfectly plastic (inelastic) collisions, so any solution trajectory intersecting this hyperplane is subjected to the discontinuous impact map $\Delta : G \to T\mathcal{Q}$. Thus, we have the *impulsive* dynamical system

$$\begin{aligned} M(\theta)\ddot{\theta} + C(\theta, \dot{\theta})\dot{\theta} + N(\theta) = Su \qquad & \text{for } (\theta, \dot{\theta}) \notin G \\ (\theta^+, \dot{\theta}^+) = \Delta(\theta^-, \dot{\theta}^-) \qquad & \text{for } (\theta^-, \dot{\theta}^-) \in G. \end{aligned}$$

For brevity we defer the impact map details to [9], [10].

Bipedal walking gaits will correspond to solutions $x(t) = (\theta(t), \dot{\theta}(t))$ of the above system that are periodic, i.e., $x(t) = x(t+T)$ for some $T > 0$ and all $t$, and therefore define closed orbits $\mathcal{O} = \{x(t) | t \geq 0\} \subset T\mathcal{Q}$. Stability of these so-called *periodic limit cycles* is determined with the *Poincaré map* $P : G \to G$, which represents an impulsive dynamical system as a discrete-time system between impact events. This map sends state $x_j \in G$ ahead one step by the discrete system $x_{j+1} = P(x_j)$. Thus, a 1-step periodic solution $x(t)$ has a *fixed-point* $x^* \in G$ such that $x^* = P(x^*)$.

Although we cannot analytically calculate this map to determine its stability about $x^*$, we can numerically approximate it through simulation. This allows us to analyze orbit stability as a linear discrete system by the map's linearization, $\delta P$. We then know that a periodic limit cycle is *locally exponentially stable* (LES) if and only if the eigenvalues of $\delta P$ are strictly within the unit circle. The local stability region about fixed-point $x^*$, known as the *basin of attraction*, is defined as

$$BoA(x^*) = \{x \in G \;\text{ s.t. }\; \lim_{k\to\infty} P^k(x) = x^*\}. \quad (10)$$

The numerical details of Poincaré analysis are given in [9].

### B. Control Strategy

In order to develop a strategy that will be effective at locomotor training, we adopt three guiding principles in the selection of desired potential energy $\widetilde{\mathcal{V}}$:

1) Satisfy energy matching condition (6).
2) Preserve the natural limit cycle known to exist in the nonlinear hybrid dynamics.
3) Alter dynamical characteristics of the human "plant" to mimic the body-weight support/stability provided by harnesses in effective gait training methods [14], [17].

Guided by inspection of full-order $N(\theta)$, we notice that hip mass $m_{\rm h}$ only appears in the first row (the other row is invariant under changes in this parameter). Moreover, the first row does not depend on $\theta_{\rm ns}$. Without much difficulty, this can be proven as a *general property* of bipedal kinematic chains when the stance knee is locked, so this also applies to more anthropomorphic models.

Therefore, we adopt $\widetilde{\mathcal{V}}$ corresponding to original potential energy (8) with a *virtual* hip mass $\widetilde{m}_{\rm h}$ of our choosing:

$$\widetilde{V}(\theta) = -\frac{1}{2}gl(m_{\rm l}\cos(\theta_{\rm ns}) - (3m_{\rm l} + 2\widetilde{m}_{\rm h})\cos(\theta_{\rm s})). \quad (11)$$

This desired potential energy has the shaped torque vector

$$\widetilde{N}(\theta) = \nabla_\theta \widetilde{V} = \begin{pmatrix} -gl(3m_{\rm l} + 2\widetilde{m}_{\rm h})\sin(\theta_{\rm s})/2 \\ glm_{\rm l}\sin(\theta_{\rm ns})/2 \end{pmatrix}. \quad (12)$$

Noting that $S^\perp = \begin{pmatrix} 0 & 1 \end{pmatrix}$, it is easy to verify that matching condition (6) always holds – potential energy $\widetilde{V}$ is indeed

[4]The dual AFO assumption could be relaxed for hemiparetic patients, possibly resulting in asymmetric walking gaits.

[5]This model does not have knees to provide ground clearance of the swing foot, so we add the tangential constraint $\dot{h} < 0$ to the condition $h = 0$ to disallow impact events associated with mid-swing scuffing [21].

within the range space of $S$. Equation (7) then yields the following control law for the underactuated (scalar) input:

$$\begin{aligned} u(\theta_{\mathrm{s}}) &= (S^T S)^{-1} S^T \left( N(\theta) - \widetilde{N}(\theta) \right) \\ &= gl(\widetilde{m}_{\mathrm{h}} - m_{\mathrm{h}}) \sin(\theta_{\mathrm{s}}). \end{aligned} \tag{13}$$

A human body's COM is approximately located at the hip. If we choose $\widetilde{m}_{\mathrm{h}} < m_{\mathrm{h}}$, this potential-shaping control provides body-weight support to make the patient feel lighter by a specified amount. We evaluate the implications this has on gait therapy in Section V. Note that by choosing $\widetilde{m}_{\mathrm{h}} > m_{\mathrm{h}}$, this instead becomes a "challenge-based" controller (the opposite of assistive), which may be more appropriate for some forms of impairment [15].

***Remark 1:*** Instead of assuming passive human walking, the unknown human control policy can be interpreted as an auxiliary control signal $v$ in the human-machine feedback loop of Fig. 2. This does not interfere with potential-shaping control (13) from the AFO – we can add negative feedback from input $v$ to the right-hand side of (4) and still obtain matching conditions (5)-(6). This allows us to draw analogies to the general case of human walking on arbitrary slopes; and by the same reasoning, an additional control term can be superimposed to compensate for specific neuromotor disorders such as weakened ankle pushoff/propulsion [4], [5].

### C. Alternate Strategies

The potential-shaping method of slope-invariant "controlled symmetries" has proven useful in finding walking gaits for various bipedal robots [10], [11], [21]. This strategy shapes the gravity vector into a virtual vector that is rotated to make any given slope (e.g., an incline) feel like an arbitrary slope of choice (e.g., a decline). However, the potential term $\widetilde{N}(\theta)$ that yields the closed-loop system slope-invariant violates matching condition (6) for $m < n$. Thus, underactuated control law (7) only provides the portion of the control within the range space of $S$. This might serve well as an *approximate* controller (and using this strategy we have indeed found stable limit cycles down slopes), but we cannot guarantee meaningful behavior. We encounter a similar problem when shaping the magnitude of gravity, but these alternate strategies may be more practical with full lower-extremity exoskeletons [22].

## V. Rehabilitation Implications

We can now draw several implications of AFO control policy (13) based on simulations and theoretical analysis.

### A. Effect on Passive Walking Gait

It is well established in the literature (e.g., [7], [9]) that passive dynamic walking gaits exist down shallow slopes for a wide variety of hip mass values. In fact, the dynamics specifically depend on the *ratio* between hip mass $m_{\mathrm{h}}$ and leg mass $m_{\mathrm{l}}$, where $\mu = m_{\mathrm{h}}/m_{\mathrm{l}}$ simply scales the gait characteristics [9]. This allows our application to be scaled to humanoid models of varying body parameters.

However, our potential-shaping policy does not change the hip mass parameter in *kinetic* energy $\frac{1}{2}\dot{\theta}^T M(\theta)\dot{\theta}$. The closed-loop swing dynamics associated with control (13) are

$$M(\theta)\ddot{\theta} + C(\theta, \dot{\theta}) + \widetilde{N}(\theta) = 0, \tag{14}$$

where $M$ depends on $m_{\mathrm{h}}$ (in only the top-left term), $C$ has no hip mass dependence, and $\widetilde{N}$ depends on $\widetilde{m}_{\mathrm{h}}$. Note that impact map $\Delta$ still depends on original parameter $m_{\mathrm{h}}$.

Two additional control components are necessary to obtain a closed-loop system equivalent to the *target* passive walker (the physical robot with *actual* hip mass $\widetilde{m}_{\mathrm{h}}$). Kinetic energy shaping would yield equivalent continuous-time dynamics, but requires a more sophisticated feedback law with additional state measurements. Impulsive control at impact events would shape the impact dynamics for dependence on $\widetilde{m}_{\mathrm{h}}$, but this is difficult to implement in practice.

Fortunately, we can show via simulation that potential shaping is practically sufficient (i.e., the difference between gaits is marginal) when imposing a moderate range of virtual masses. Recall that gravitational potential energy is the "power source" behind passive dynamic walking. The *shaped* potential energy (with respect to virtual mass $\widetilde{m}_{\mathrm{h}}$) at the beginning of each passive gait cycle is converted into kinetic energy (with respect to actual mass $m_{\mathrm{h}}$) by the end of each passive gait cycle. Therefore, we assert that the augmented gait will closely resemble that of the target passive walker.

In order to ensure the existence of passive walking gaits in our analysis, we adopt common parameters $\mu = 2$, $l = 1$ m (roughly approximating a human without a torso) from [9]–[11]. The evolution of stable fixed-points corresponding to both the target and AFO-emulated gaits on a decline slope of angle $\gamma = \pi/50$ are compared in Fig. 3 over values $\widetilde{m}_{\mathrm{h}} \in [0.2, 10]$ (initial $m_{\mathrm{h}} = 10$ kg). The gait characteristics of limit cycle energy,[6] stride length, and linear velocity are shown over this range in Fig. 4. The total energy of each system's limit cycle evolve very closely over the entire range, whereas the step length diverges slowly and the step velocity diverges only for very small masses ($\widetilde{m}_{\mathrm{h}} < 4$ kg).

An important difference regarding stability is seen in Fig. 5, where the numerically computed eigenvalues are smaller in the shaped passive system than the target passive system for $\widetilde{m}_{\mathrm{h}} > 4$ kg. Over this range, the maximum eigenvalue of the shaped passive system decreases almost linearly as $\widetilde{m}_{\mathrm{h}}$ decreases, suggesting that the AFO-assisted system is more robust to gait perturbations. However, these eigenvalues only reflect the local behavior of this highly nonlinear system.

Based on these simulations, we can predict that the AFO strategy would slow a patient's walking gait, decreasing overall system energy. Much like a body harness, this improves gait stability by preventing explosions in system energy that lead to falling. This allows safe training toward progressively faster and more natural walking gaits, which we discuss in

[6]By conservation of energy for physical systems, the target walker will have *constant* energy along any 1-step periodic limit cycle. The shaped system is not equivalent to any physical system, so although we cannot guarantee energy conservation during swing phase, simulations show the energy level to be *nearly constant* and certainly *periodic* along limit cycles.

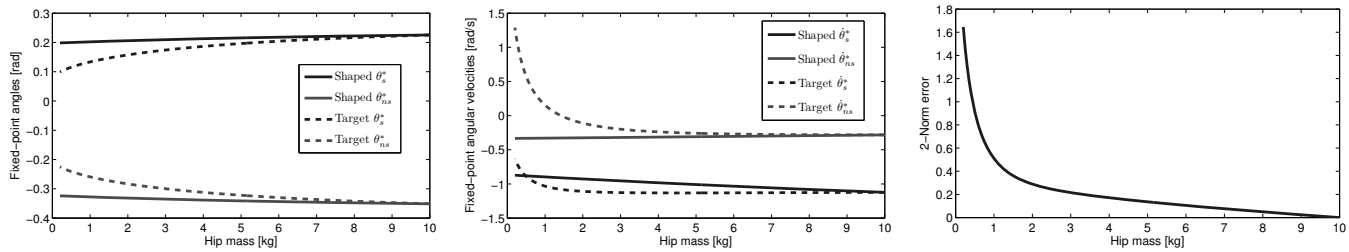


Fig. 3. Comparing the *shaped* passive walker (with virtual hip mass $\widetilde{m}_{\mathrm{h}}$ in potential energy and original mass $m_{\mathrm{h}} = 10$ kg in kinetic energy) against the *target* passive walker with actual hip mass $\widetilde{m}_{\mathrm{h}}$ down slope $\gamma = \pi/50$: fixed-point angles (left), fixed-point angular velocities (middle), and 2-norm error between the two system fixed-points (right) plotted against $\widetilde{m}_{\mathrm{h}}$.

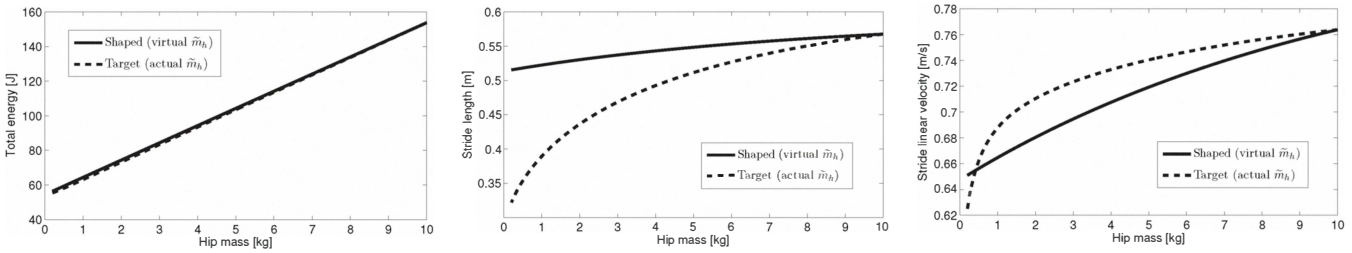


Fig. 4. Comparing the *shaped* passive walker against the *target* passive walker down slope $\gamma = \pi/50$: total limit cycle energy (left), stride length (middle), and stride linear velocity (right) plotted against $\widetilde{m}_{\mathrm{h}}$.

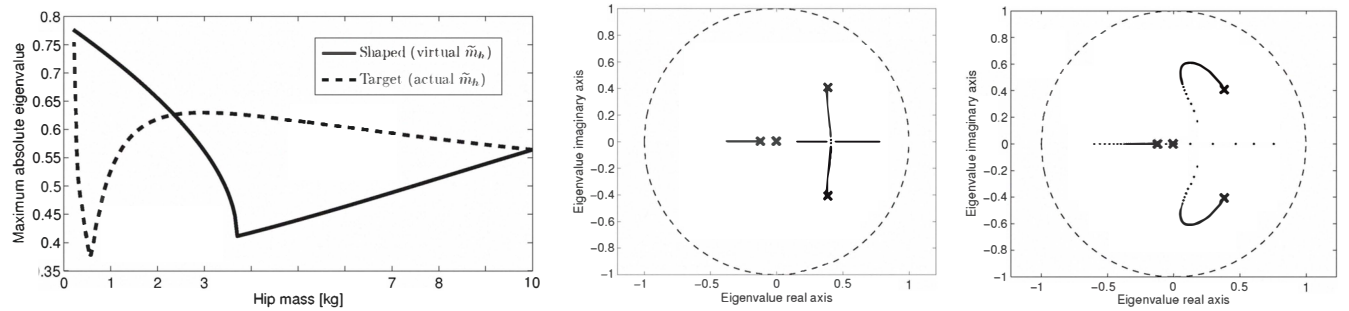


Fig. 5. Comparing both systems walking down slope $\gamma = \pi/50$: maximum absolute eigenvalues against $\widetilde{m}_{\mathrm{h}}$ (left) and the corresponding root locus plots of the *shaped* passive walker (middle) and the *target* passive walker (right).

Section V-D. Although the above example only considers decline walking, this strategy would preserve any limit cycle existing in the hybrid dynamics.

### B. Effect on Phases of Human Walking Cycle

The double-support phase of a human gait cycle (Fig. 6) includes a pushoff period (positive COM work) followed by collision/weight-acceptance (negative COM work) [24]. However, the passive compass-gait biped has instantaneous double-support due to rigid impacts (negative work) and immediate replenishment of potential energy by the decline slope (positive work). A human's support foot is only flat during midstance, so our assumed contact constraint for applying ankle torques against ground is only valid during this phase. Therefore, the compass-gait model is most useful for describing the midstance behavior of human walking, which begins with "rebounding" during the upward pendular arc (positive COM work) and ends with "preloading" during the downward arc (negative COM work).

The torque and power profiles for one augmented passive gait is shown in Fig. 7. We see that each leg's AFO performs positive work during rebound followed by negative work during preload. I.e., the AFO strategy assists the Achilles tendon in storing "elastic" energy during preloading, but releases this energy during rebound rather than pushoff. As we would expect, the torques contributed by the AFO do not resemble those of a human walking gait. Although assistive control strategies (e.g., those based on reference trajectories/patterns) commonly attempt to provide human-like torques, we argue that strategies should instead enable and encourage the *human* to do this. Our approach is further distinguished by the fact that active control during midstance is uncommon in existing AFO control strategies (e.g., [5]), presumably because a human's stance ankle behaves passively during this phase.

### C. Energetic Consequences

Integrating instantaneous power $\dot{\theta}_{\mathrm{s}} u$, we find that the AFO performs net $1.691$ J of negative mechanical work (specific average power is $-0.111$ W/kg) to shape the hip mass to

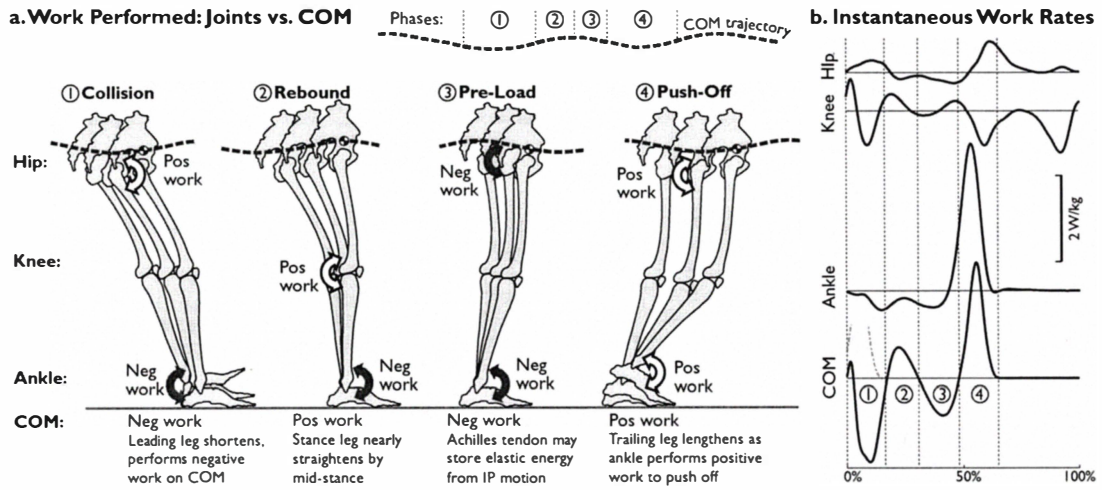


Fig. 6. Diagram of the stance phase of a human walking gait. Part (a) illustrates the four subphases known as collision/weight-acceptance, rebound, preload, and pushoff, also indicating the work performed by each lower-extremity joint in comparison with the COM. Part (b) plots the instantaneous power for each joint and the COM over an entire gait cycle (based on empirical data from [23]). Reproduced from [24] with permission from the publisher.

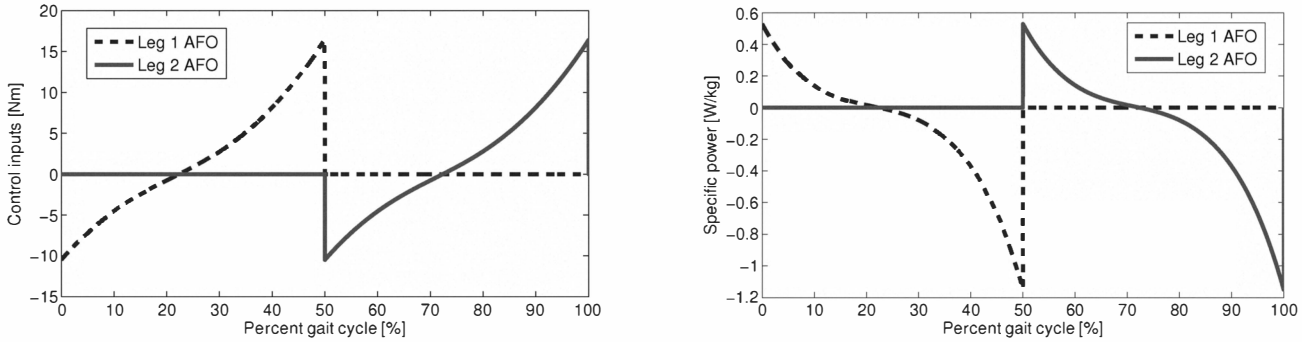


Fig. 7. Each leg's AFO input torque (left) and specific instantaneous power (right) for two steps along limit cycle of the shaped passive biped ($\widetilde{m}_{\mathrm{h}} = 5$ kg, $m_{\mathrm{h}} = 10$ kg, $\gamma = \pi/50$). Recall that these are consequences of feedback law (13) rather than any reference trajectory.

$\widetilde{m}_{\mathrm{h}} = 5$ kg throughout one step cycle. The AFO performs more negative work than positive work because of the decline slope, where extra potential energy must be absorbed to mimic the smaller hip mass. Net mechanical work would be near zero on level ground, as the positive work needed to counteract gravity during the hip's upward pendular arc approximates the negative work needed to slow the gravity-induced downward arc.

For the human application, we must consider the nontrivial pushoff period at the end of stance phase, when the support ankle is raised up to 15 degrees from ground and briefly performs a significant amount of positive work. We see in Fig. 7 that our control policy would attempt to perform negative work at the ankle during this period, which may feel like resistance to the patient's pushoff. In some cases, this form of resistance may be helpful for locomotor training. In other cases, the AFO could superimpose a common pushoff-assist torque profile.

Due to energy redirection during midstance, patient pushoff will be easier with or without pushoff assistance. The mechanical work done by each leg primarily serves to redirect the pendular trajectory of the body's COM during step transitions (i.e., double support), and this work quantity is shown to be proportional to the total body mass in [24]:

$$W_{\mathrm{leg}} \propto M_{\mathrm{tot}}(v_{\mathrm{com}}^{-}\tan(\alpha))^2, \tag{15}$$

where $v_{\mathrm{com}}^{-}$ is the linear COM velocity just prior to ground impact, $\alpha$ is the inner-leg angle at impact, and in our case

$$M_{\mathrm{tot}} = m_{\mathrm{h}} + 2m_{\mathrm{l}}.$$

Given our AFO control strategy, the human work contribution will instead be proportional to

$$\widetilde{M}_{\mathrm{tot}} = \widetilde{m}_{\mathrm{h}} + 2m_{\mathrm{l}}.$$

Choosing $\widetilde{m}_{\mathrm{h}} < m_{\mathrm{h}}$, we reduce the human effort during double support by roughly

$$(M_{\mathrm{tot}} - \widetilde{M}_{\mathrm{tot}})/M_{\mathrm{tot}}.$$

Hence, the strategy provides assistance during single support so that the human subject feels lighter during double support.

### D. Progressive Training by Lyapunov Funneling

Body-weight assistance is commonly given to paretic patients during locomotor training to compensate for neuromuscular weakness. This support also results in gaits with *smaller* step lengths and velocities (Fig. 4) that are initially easier to produce. At the onset of AFO therapy, control parameter $\widetilde{m}_{\mathrm{h}}$ can be initialized small and gradually tuned towards $m_{\mathrm{h}}$ as the patient's locomotor skills improve (approaching no assistance). This process of sequentially composing controllers to stably achieve intermediate training gaits is known as *Lyapunov funneling* (cf. [25] or the robot walking applications of [26], [27, Ch. 4.6.1]).

Given an initial choice $\widetilde{m}_{\mathrm{h}}^1$, the human subject engages in AFO-assisted training to learn the corresponding walking gait (which might first involve manual assistance or support rails). In other words, the state of the closed-loop discrete system corresponding to the assisted human gait converges toward LES fixed-point $x_1^*$ with $BoA(x_1^*)$ from (10). The next parameter $\widetilde{m}_{\mathrm{h}}^2$, where $\widetilde{m}_{\mathrm{h}}^2 > \widetilde{m}_{\mathrm{h}}^1$, must then be chosen to allow safe and easy transition to the next intermediate gait. Starting from the first gait (initial condition $x_1^*$), the patient will stably converge toward the new gait corresponding to $x_2^*$ if $x_1^* \in BoA(x_2^*)$. For $\widetilde{m}_{\mathrm{h}}^2$ sufficiently close to $\widetilde{m}_{\mathrm{h}}^1$, this funneling condition is assured by the continuous dependence of $x^*$ and $BoA(x^*)$ on the virtual hip mass.

This process can be repeated several times as $\widetilde{m}_{\mathrm{h}}^i \to m_{\mathrm{h}}$, where the patient gradually gains strength and confidence until some nominal walking gait is acquired. The simulations of Fig. 4 suggest that this progressively increases the step length and velocity (funneling would move positively along the $x$-axis), which we would expect to accompany gait rehabilitation. However, the divergence of the AFO-emulated walking gait from the target walking gait for small virtual masses (e.g., $\widetilde{m}_{\mathrm{h}} < 4$ kg) may constrain the initial choice $\widetilde{m}_{\mathrm{h}}^1$ of the progressive training regiment.

This framework may enable physical therapists to design sequences of intermediate training gaits to treat patient-specific impairments. Performance-based adaptation of $\widetilde{m}_{\mathrm{h}}$ could further ensure the patient is always sufficiently challenged throughout training, which is thought to be critical to neuro-rehabilitation [15].

### E. Implementation Remarks

As opposed to strategies that execute predefined torques based on the percentage of the gait cycle, control law (13) requires no modal estimation of gait phase or user intent. This strategy's torques are defined in terms of feedback from angular *position* $\theta_{\mathrm{s}}$, the orientation of stance leg with respect to ground. This state can be measured easily from the AFO, requiring no sensors on the patient's body. The control law depends only on the *difference* between actual and virtual masses, $\delta m_{\mathrm{h}} = m_{\mathrm{h}} - \widetilde{m}_{\mathrm{h}}$, so the policy can be simply defined in terms of the desired amount of body-weight support. The only other parameter needed is the leg length, making this strategy easily tuned to individual morphology.

A well-designed AFO (e.g., the fluid-powered device in [5]) can efficiently harvest energy – in our case, storing energy during preload for release during rebound. The robotic device must be backdriveable with low friction, so as not to dampen the ballistic motion of the patient. Friction would enter into the right-hand side of closed-loop dynamics (14) and dissipate energy through the entire walking cycle.

Input clipping must also be avoided for these single-support dynamics to hold, so it is beneficial to determine the controllable range of hip masses for a given torque bound $U_{\max}$. Conservatively assuming that $|\theta_{\mathrm{s}}| \leq \pi/6$ (thus $|\sin(\theta_{\mathrm{s}})| \leq 1/2$), we can show the following upper bound on body-weight support:

$$\begin{aligned} |u(\theta_{\mathrm{s}})| &\leq gl|\delta m_{\mathrm{h}}|/2 \leq U_{\max} \\ \implies |\delta m_{\mathrm{h}}| &\leq \frac{2U_{\max}}{gl}. \end{aligned}$$

It is important to recall that this holds independent of the absolute mass of the subject, so we can relate this to our example model or a real human subject.

If we choose $U_{\max} = 20$ Nm for our model, then any $|\delta m_{\mathrm{h}}| \leq 4.08$ kg will be within the saturation bounds. Note that all gaits in Fig. 3 have $|\theta_{\mathrm{s}}| \leq \pi/10$, implying the more liberal bound $|\delta m_{\mathrm{h}}| \leq 6.6$ kg. The prototype PPAFO from [5] has $U_{\max} = 10$ Nm, which would instead provide $|\delta m_{\mathrm{h}}| \leq 3.3$ kg for a human subject with $l = 1$ m. Given that healthy humans peak at ankle torques around 130 Nm [28], future PPAFO iterations will allow stronger torque profiles for increased body-weight support.

## VI. Conclusions and Future Work

This paper proposed a novel control theoretic strategy for AFO gait assistance based on underactuated potential energy shaping. More generally, this offers a systematic approach to control strategy design for locomotor rehabilitation, where meaningful characteristics of the human "plant" are modified for therapeutic value using a simple feedback loop *without* reference trajectories. Such strategies are independent of gait modality (e.g., walking, standing, or climbing stairs) and thus inherently compliant to patient intent.

This design methodology enables a theoretical framework for progressive locomotor therapy, where the human-AFO system is sequentially funneled toward the nominal walking gait (preventing patient dependence on the physical assistance). The natural walking demonstrated by our passive walking model may motivate additional studies on locomotor training by funneling decline gaits toward flat ground gaits.

The control strategy developed in this paper was shown to improve the stability of passive walking gaits, suggesting application to PPAFO devices for at-home assistance of the disabled or elderly. This also offers a simple approach to exoskeletal performance augmentation (cf. [22]) for carrying heavy equipment near the body's COM, where the virtual mass can be tuned to the human's mass without payload.

We are currently investigating experimental applications of this strategy on the PPAFO from [5]. We make no claims that this alone will suffice for effective rehabilitation, but we have offered a meaningful design methodology that can be refined based on practical and clinical considerations.

*Acknowledgments*

We thank Elizabeth Hsiao-Wecksler, Alex Shorter, and Aaron Becker for helpful discussions about the Illinois PPAFO and common control methods for gait assistance.

## REFERENCES

[1] H. I. Krebs and N. Hogan, "Therapeutic robotics: A technology push," *Proc. of the IEEE*, vol. 94, no. 9, p. 1727, 2006.

[2] T. Hornby, D. Campbell, J. Kahn, T. Demott, J. Moore, and H. Roth, "Enhanced gait-related improvements after therapist-versus robotic-assisted locomotor training in subjects with chronic stroke: a randomized controlled study," *Stroke*, vol. 39, no. 6, pp. 1786–1792, 2008.

[3] J. Hidler, D. Nichols, M. Pelliccio, K. Brady, D. Campbell, J. Kahn, and T. Hornby, "Multicenter randomized clinical trial evaluating the effectiveness of the lokomat in subacute stroke," *Neurorehabilitation and Neural Repair*, vol. 23, no. 1, p. 5, 2009.

[4] A. Roy, H. Krebs, D. Williams, C. Bever, L. Forrester, R. Macko, and N. Hogan, "Robot-aided neurorehabilitation: A novel robot for ankle rehabilitation," *IEEE Trans. Robotics*, vol. 25, pp. 569–582, 2009.

[5] R. Chin, E. T. Hsiao-Wecksler, E. Loth, G. Kogler, S. D. Manwaring, S. N. Tyson, K. A. Shorter, and J. N. Gilmer, "A pneumatic power harvesting ankle-foot orthosis to prevent foot-drop," *J. of NeuroEngineering and Rehabilitation*, vol. 6, no. 1, p. 19, 2009.

[6] A. D. Kuo, "Choosing your steps carefully: walking and running robots," *IEEE Robotics and Automation Mag.*, vol. 14, no. 2, pp. 18–29, 2007.

[7] T. McGeer, "Passive dynamic walking," *Int. J. of Robotics Res.*, vol. 9, no. 2, pp. 62–82, 1990.

[8] S. H. Collins, M. Wisse, and A. Ruina, "A 3-D passive dynamic walking robot with two legs and knees," *Int. J. of Robotics Res.*, vol. 20, pp. 607–615, 2001.

[9] A. Goswami, B. Thuilot, and B. Espiau, "Compass-like biped robot part I: Stability and bifurcation of passive gaits," Institut National de Recherche en Informatique et en Automatique, Tech. Rep. 2996, 1996.

[10] M. W. Spong, "The passivity paradigm in bipedal locomotion," in *Int. Conf. on Climbing and Walking Robots*, Madrid, Spain, 2004.

[11] M. W. Spong and F. Bullo, "Controlled symmetries and passive walking," *IEEE Trans. Automatic Control*, vol. 50, no. 7, pp. 1025–1031, 2005.

[12] W. R. Leonard and M. L. Robertson, "Energetic efficiency of human bipedality," *Amer. J. of Phys. Anthro.*, vol. 97, pp. 335–338, 1995.

[13] A. E. Minetti, C. Moia, G. S. Roi, D. Susta, and G. Ferretti, "Energy cost of walking and running at extreme uphill and downhill slopes," *J. of Applied Physiology*, vol. 93, no. 3, p. 1039, 2002.

[14] S. Hesse, C. Werner, T. Paul, A. Bardeleben, and J. Chaler, "Influence of walking speed on lower limb muscle activity and energy consumption during treadmill walking of hemiparetic patients," *Arch. of Phys. Medicine and Rehab.*, vol. 82, no. 11, pp. 1547–1550, 2001.

[15] L. Marchal-Crespo and D. Reinkensmeyer, "Review of control strategies for robotic movement training after neurologic injury," *J. of NeuroEngineering and Rehabilitation*, vol. 6, no. 1, p. 20, 2009.

[16] H. Vallery, A. Duschau-Wicke, and R. Riener, "Generalized elasticities improve patient-cooperative control of rehabilitation robots," in *IEEE Int. Conf. on Rehab. Robotics*, Kyoto, Japan, 2009, pp. 535–541.

[17] M. Frey, G. Colombo, M. Vaglio, R. Bucher, M. Jorg, and R. Riener, "A novel mechatronic body weight support system," *IEEE Trans. Neural Systems and Rehab. Eng.*, vol. 14, no. 3, pp. 311–321, 2006.

[18] S. Agrawal, S. Banala, A. Fattah, V. Sangwan, V. Krishnamoorthy, J. Scholz, and W. Hsu, "Assessment of motion of a swing leg and gait rehabilitation with a gravity balancing exoskeleton," *IEEE Trans. Neural Systems and Rehab. Eng.*, vol. 15, no. 3, pp. 410–420, 2007.

[19] R. Ortega, M. W. Spong, F. Gomez-Estern, and G. Blankenstein, "Stabilization of a class of underactuated mechanical systems via interconnection and damping assignment," *IEEE Trans. Automatic Control*, vol. 47, no. 8, pp. 1218–1233, 2002.

[20] A. M. Bloch, D. E. Chang, N. E. Leonard, and J. E. Marsden, "Controlled Lagrangians and the stabilization of mechanical systems. II: Potential shaping," *IEEE Trans. Automatic Control*, vol. 46, no. 10, pp. 1556–1571, 2001.

[21] R. D. Gregg and M. W. Spong, "Reduction-based control of three-dimensional bipedal walking robots," *Int. J. of Robotics Research*, vol. 26, no. 6, pp. 680–702, 2010.

[22] H. Kazerooni, "Exoskeletons for human performance augmentation," in *Handbook of Robotics*. New York, NY: Springer, 2008, pp. 773–793.

[23] D. A. Winter, *Biomechanics and Motor Control of Human Movement*. Hoboken, NJ: Wiley, 2009.

[24] A. D. Kuo, J. M. Donelan, and A. Ruina, "Energetic consequences of walking like an inverted pendulum: step-to-step transitions," *Exercise and Sport Sciences Reviews*, vol. 33, no. 2, pp. 88–97, 2005.

[25] R. Burridge, A. Rizzi, and D. Koditschek, "Sequential composition of dynamically dexterous robot behaviors," *Int. J. of Robotics Res.*, vol. 18, no. 6, pp. 534–555, 1999.

[26] R. D. Gregg, T. W. Bretl, and M. W. Spong, "Asymptotically stable gait primitives for planning dynamic bipedal locomotion in three dimensions," in *IEEE Int. Conf. on Robotics and Automation*, Anchorage, AK, 2010, pp. 1695–1702.

[27] E. R. Westervelt, J. W. Grizzle, C. Chevallereau, J. H. Choi, and B. Morris, *Feedback Control of Dynamic Bipedal Robot Locomotion*. New York, NY: CRC Press, 2007.

[28] M. D. Sockol, D. A. Raichlen, and H. Pontzer, "Chimpanzee locomotor energetics and the origin of human bipedalism," *Proc. of the National Academy of Sciences*, vol. 104, no. 30, pp. 12 265–12269, 2007.